CASE STUDY // TURBO MACHINERY

INCREASED EFFICIENCY BY OPTIMIZING THE LAST STAGE OF A STEAM TURBINE

A large gain in efficiency is expected from the optimization of the last stage and the following diffuser of a low pressure turbine (LP) by minimizing losses due to separations as well as inefficient blade or diffuser designs.

Introduction

The energy supply now and in the future is one of the most important issues of our time. It is foreseeable that in the future the energy consumption continues to rise and the supply of coal and other fossil fuels worldwide will decrease. In order to meet future energy needs, in addition to the development of new renewable energy sources, the existing methods for energy production must be as efficient as possible. Further development and the use of modern technologies in power plants, as well as new computational methods for the optimization of turbo machinery, are options for a more economical use of the existing energy resources. But not only increasing the efficiency is one of the key criteria in today's turbo machinery development, in the case of electricity generation mainly the reduced emission of pollutants and, thus, the preservation of the environment, represents an increasingly significant role.

Time efficient optimization methods, as presented here, and the increasing power of computers, make it possible to increase efficiency, which makes it possible to produce more energy under the same amount of resources and, thus, a reduction of pollution compared to a less efficient production.

This article describes an optimization of the last stage of a low pressure steam turbine followed by a diffuser. Since more than 30% of the power is produced in the last two stages of the turbine, this part provides great potential for improving the efficiency of the cold end of the turbine. The resulting losses may be reduced only to a lesser extent by a heat recovery. Therefore, the optimization of the outflow and the conversion of kinetic energy into potential energy by improving the pressure recovery in the diffuser, can decrease the enthalpy at the outlet of the diffuser and so increase the enthalpy difference and thus also significantly improve the system efficiency.

A decisive factor for optimizing this components is the joint consideration of both the last stage and the diffuser. In most cases, the respective components are designed and optimized separately and therefore the full potential for optimization is left aside. Therefore, it will be presented in this article, first a sequential optimization of the last stage followed by a optimization of the diffuser. In comparison, a coupled optimization of both components will be made to show the differences between these two methods. As a basis for this work, their is a self-made design of a last stage and the diffuser based on information of the industry and literature. In the simulation, next to the flow simulation, a mechanical and dynamical analysis of the stresses and natural frequencies is performed. The calculations are conducted using ANSYS Workbench software. In the first step of optimization, using the optimization software optiSLang, the blades are optimized for fixed diffuser parameters. In the second step, the optimized blades are also fixed and the diffuser is optimized. In the final step, a coupled optimization of diffuser and blades is carried out, starting from the initial design. In the coupled optimization a large number of parameters for both components (51 overall) is involved to also represent the opportunities to solve any large optimization problems efficiently. By the individual optimizations, the sensitive parameters and correlations for the respective outputs and components are also noted.

In the field of optimization of the coupled last turbine stage and the subsequent diffuser, there are already some publications. In most cases, however, the calculations are carried out using 2D codes in order to avoid the high computational cost of 3D simulation. With the constant improvement of computer power and more efficient numerical method, it is worthwhile to work on this topic in the 3D area more and more. Overall, all these publications show a clear improvement over the outcome designs that are previously developed sequential.

Application to aerodynamic optimization

In comparative studies on the application of the deterministic optimization for aerodynamic optimization *Müller-Töws (2000); Sasaki et al. (2001); Shahpar (2000)* usually stochastic programming algorithms or response surface methods *Pierret and Van den Braembussche (1999)* are used in turbo machinery design, for example in the development of engine components, such as at *Vaidyanathan et al. (2000)*. In *Shyy et al. (2001)* a comprehensive overview is represented.

An example of an applied aerodynamic deterministic optimization using a genetic algorithm is published in *Trigg et al. (1997)* and the optimized design of transonic profiles also using genetic algorithms is given in *Oyama (2000)*. Another very comprehensive study of the use of the combination of genetic algorithms and neural networks for two dimensional aerodynamic optimization of profiles is presented in *Dennis et al. (1999)*, who combined a genetic algorithm with an gradient based optimization method.

Application to coupled optimization of the last stage and successive diffuser

One of the first works in this area was published in *Willinger (1997)* in 1997. The aim of this work was not to optimize the coupled components, but in general, to determine the interaction of both components. In particular, the radial gap between rotor and casing was varied, while they observed improvements in the pressure recovery in the diffuser. With increasing the radial gap, the pressure recovery was improved, but with greater flow losses. These losses could not be outweighed by the greater pressure recovery. By increasing the marginal gap, the gap current experiences more energy which allows for certain construction of the diffuser to avoid separations. In particular this has the advantage that shorter lengths of the diffuser are possible, as well as greater diffuser opening ratio. Similarly, in this work, the proposal will be given a numerical optimization to determine further interaction phenomena and to integrate them into the optimization. Also *Jung (2000)* initially dealt only with the phenomena that occur in a coupled calculation and developed in his work an efficient numerical method for the calculation of the coupled model. An optimization is presented for example in *Kreitmeier and Greim (2003)* using a low pressure turbine stage and a subsequent axial radial diffuser. Here, the diffuser has been optimized under fixed blade geometry. The optimization was carried out using a numerical method and in a second sample using an experimental optimization. Both methods achieved significantly better performance than comparable standard designs. The best result came from a 3 channel diffuser. Further work on this area was performed by *Fan et al. (2007)* in a coupled optimization. It turned out that the inhomogeneous flow of the output stage are one of the main reasons for separations in the diffuser. By optimizing the coupled system, also a much better overall performance was achieved. In *Stüer and Musch (2008)* a coupled optimization is also carried out with the focus on the influences of the tip jet, the influence of the flow on the diffuser is investigated with the background of the CO_2 reduction. One result of this work was the development of an efficient method for determining the release tilt of the diffuser, which makes, coupled with an optimizer, very quickly a streamlined design of a diffuser possible. One of the probably most recent work in this area represents *Musch et al. (2013)*. In this work, both last stage and diffuser, were optimized using a "covariance matrix adaptation". To reduce the high computational complexity of this optimization a 2D through-flow code called "'SLEQ'" by *Denton (1978)* was first used and then were the results validated in a further step using a 3D simulation. Result of this work was that a significantly greater potential exists for a coupled optimization. The physical explanation for this greater potential lays in the fact, that the pressure distribution in the outlet of the last stage is the inlet pressure distribution of the diffuser. Therefore, it was also recognized that diffusers, which are based on standard correlations, always lead to a not fully utilized overall performance. A similar work can be found in *Burton et al. (2012)*.

Numerical Model and Simulation

For this work a geometry of the last stage and the diffuser was made based on information from industry. The first developed model was improved by hands, until it was nearly comprehensive with machines in the industry, so that the optimization is also in an area of practical importance.

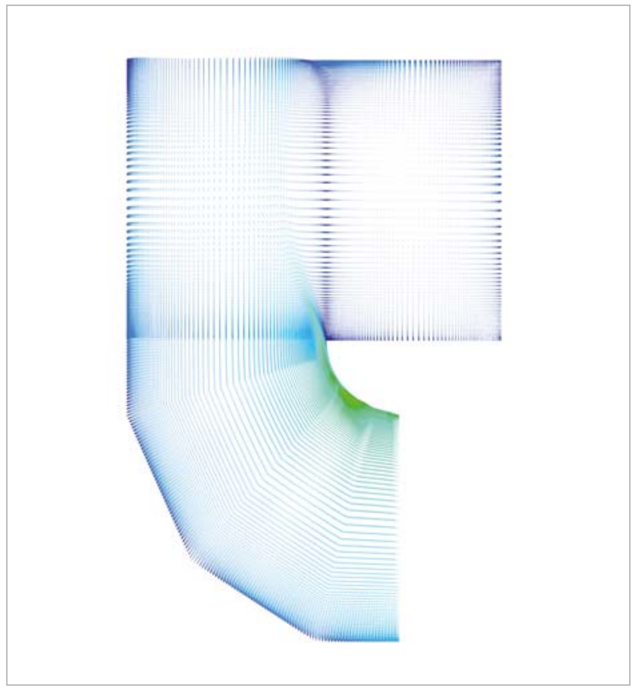

Fig. 1: Velocity profile of the initial diffuser

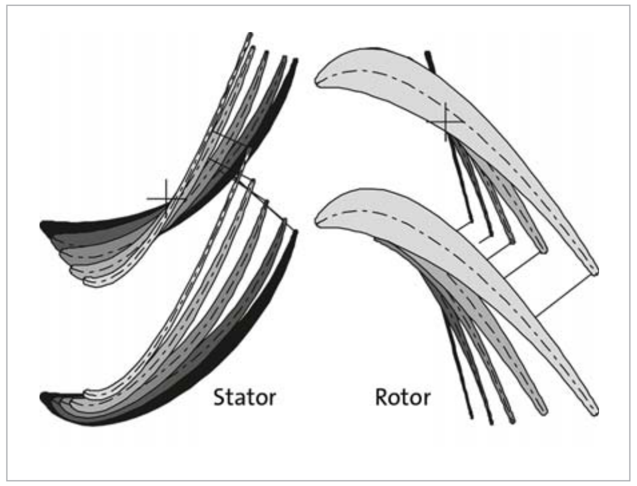

Fig. 2: Geometry of the profiles for stator and rotor

Therefore the guidelines from *Wilson and Korakianitis (1998)* were used to get a first acceptable model of the last stage. In fact that in *Wilson and Korakianitis (1998)* 16 parameters are used to describe a blade section and in ansys bladegen, which was used for the geometry creation in the simulation, only 8 parameters are possible to define, there was a transfer needed to rebuild the model in ansys bladegen with these 8 parameters shown in Fig. 2. As it is shown, the rotor hub profile is more like a reaction type blade then a typical low degree reaction type blade, which is more often used for low pressure steam turbine blades. The advantage of this is that the friction losses in the boundary layers are relatively low at this section. But this was not the main reason for this type of geometry, in the development of the blades, it comes to separations in this area if the reaction type was lower as it is shown in 2. The result is that there is high gradient for the velocity and pressure from hub to shroud, which can be seen in 11 and 13. In real applications it would be a more uniform distribution.

The same process has been done for the diffuser, which was also build up on information of the industry. There is a simplification made for the diffuser, so that it is axis symmetric. Real used diffusers are not axis symmetric because they have a different geometry in the direction of the condenser. That means for the flow simulation that also the calculated flow is axis symmetric in the diffuser, normally it would be a more complex 3-dimensional flow field. But in this case this simplification also reduces the needed calculation time. In Fig. 1 is shown the 2-dimensional velocity profile of the diffuser of the initial design.

Based on a fully parametric geometry model the software ANSYS Turbogrid and ANSYS Meshing is used to realized an automatic mesh generation with in mean 1.5 mio. hexahedron elements for the last stage used and 180k elements for the diffuser. The CFD simulation is realized by the ANSYS CFX solver in combination with mechanical and dynamic analysis for further restrictions in the optimization with 57k tetrahedra elements in the mean.

The boundary conditions for the CFD simulations, are also based on requirements of the industry. It is performed a steady state analysis with a k- turbulence model and a "total energy" heat transfer model. The used fluid is steam without wetness effects. For the inlet of the stage a pressure profile combined with a velocity profile from a real existing low pressure turbine was defined. Also the static temperature of 320 K was set. The setting for the turbulences

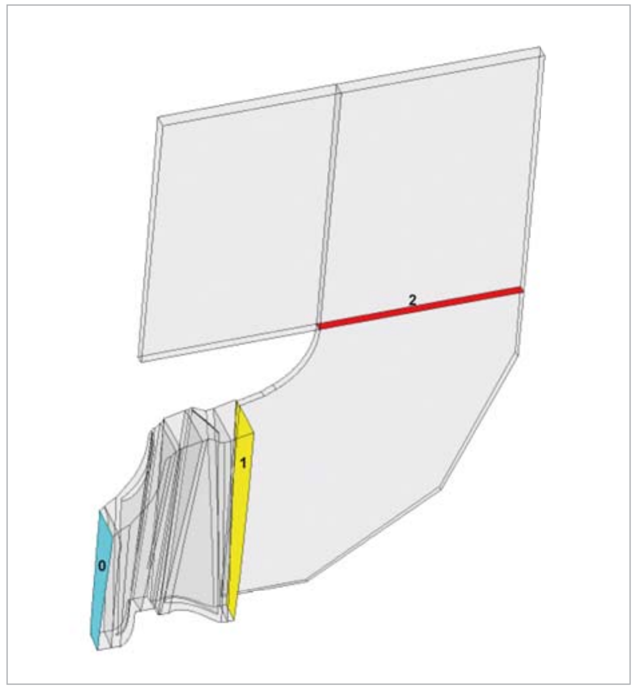

Fig. 3: Used section 0, 1, 2 for the calculation of the output variables

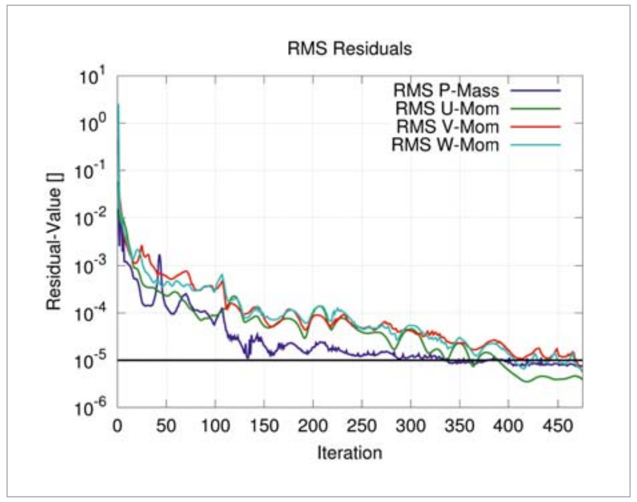

Fig. 4: RMS residuals of the CFD simulation.

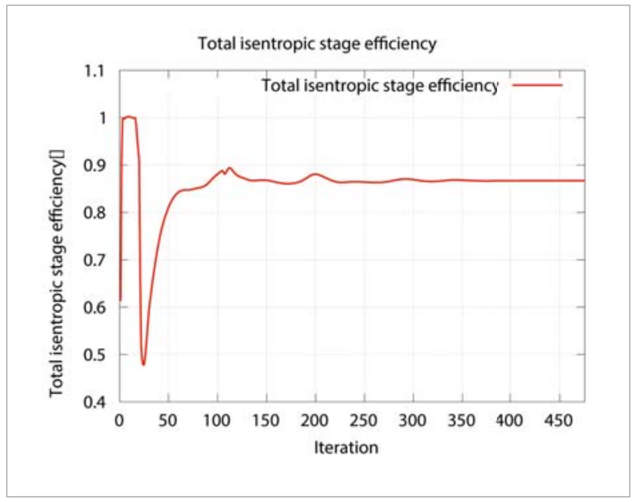

Fig. 5: Convergence of the total isentropic stage efficiency

in the inlet was medium intensity (5%). In the outlet the condenser pressure was 5.500 Pa. For the interface between stator/rotor and rotor/diffuser there was used the mixing model "'stage"'. The stage model uses the averaged circumferential flow informations, so that there is a 2-dimensional flow field information transferred to the diffuser. So there is a 3D model for one pitch length for the stage with periodic boundary conditions and a 2D model for the diffuser with rotational symmetry. The rotor tip jet is also considered due to the fact, that it has a high influence on the diffuser especially on possible separation effects. The used sections to calculate the output values are shown in Fig. 3, according to the indices 0, 1, 2 in the formulas of the outputs.

For the mechanical and dynamical boundary conditions the rotation speed is equal to 50 s–1. The influences of the pressure and temperature of the CFD analysis were not considered, because they are marginal next to the influence of the centrifugal force. The material used for the blades was X5CrNiCuNb16-4 (Material specs from Edelstahlwerke (2008)). In Fig. 4 shows the convergence of the RMS residuals. After nearly 500 Iterations the residuals confirm the stop criteria of 1e-5, according to Ansys (2012), this represents a sufficiently good convergence for such applications. For the optimization different output values are used as optimization objective or as restrictions, which are shown in the tabs. 2, 4, 5. Next to the RMS residuals there were also proved that the output parameters reach a convergent result, for example shown for the total isentropic stage efficiency in Fig. 5.

Optimization

Optimization process

Optimization is defined as a procedure to achieve the best outcome of a given objective function (sometimes also called cost function) while satisfying certain restrictions.

The deterministic optimization problem:

$$
\begin{aligned}
f(d_1, d_2, \dots d_{n_d}) &\rightarrow \min \\
e_l(d_1, d_2, \dots d_{n_d}) &= 0;\; l = 1, n_e \\
u_m(d_1, d_2, \dots d_{n_d}, \boldsymbol{\gamma}) &\geq 0;\; m = 1, n_u \\
d_{l_i} \leq d_i &\leq d_{u_i} \\
d_i \in [d_{l_i}, d_{u_i}] &\subset \mathbb{R}^{n_d}
\end{aligned}
$$

is defined by the objective function $f : \mathbb{R}^{n_d} \rightarrow \mathbb{R}$ subject to the restrictions, defined as equality and inequality constraints e_l and u_m. The variables $d_1, d_2, \dots d_{n_d}$ are the optimization or design variables and the vector of the partial safety factors γ ensures the system or design safety within the constraint equations u_m, for example defining a safety distance $u(\mathbf{d}, \gamma) = y_g/\gamma - y_d \geq 0$ between a defined limit state value y_g and the nominal design value y_d of a physical response parameter $y = f(\mathbf{d})$. In structural safety assessment, a typical constraint for the stress is given as

$$u(\mathbf{d}, \gamma) = \sigma_{y,k}/\gamma - \sigma_d \geq 0$$

ensuring the global safety distance

$$\Delta_\gamma = \sigma_{y,k}\left(1 - \frac{1}{\gamma}\right)$$

between the defined quantile value $\sigma_{y,k}$ of the yield stress and the nominal design stress σ_d with the global safety factor γ. Whereby, in the real approach with given uncertainties, σ_d corresponds to the mean of Mises equivalent stress $\bar{\sigma}_e$ at the current design point.

Global variance-based sensitivity analysis

A global variance-based sensitivity analysis, as introduced in *Saltelli et al. (2008)*, can be used for ranking variables $x_1, x_2, \dots, x_{n_r}$ with respect to their importance for a specified model response parameter

$$y = f(x_1, x_2, \dots, x_n)$$

depending on a specific surrogate model $\tilde{y}$. In order to quantify and optimize the prognosis quality of these meta-models, in *Most and Will (2012)* the so called Coefficient of Prognosis

$$\mathrm{CoP} = 1 - \frac{\mathrm{SSEP}}{\mathrm{SST}} \quad 0 \le \mathrm{CoP} \le 1$$

of the meta-model is introduced. In contrast to the commonly used generalized coefficient of determination R^2 which is based on a polynomial regression model, in this equation, variations of different surrogate models $\tilde{y}$ are analysed to maximize the coefficient of prognosis themselves. In the equation above, SSEP is the sum of squared prediction errors. These errors are estimated based on cross validation and gives some indication of the predictive capability of the surrogate model. SST is the sum squares and the equivalent to the total variation. This procedure results in the so called Metamodel of Optimal Prognosis, used as surrogate model $\tilde{y}$ with the corresponding input variable subspace which gives the best approximation quality for different numbers of samples, based on a multi-subset cross validation obtained by latin hypercube sampling *Huntington and Lyrintzis (1998)*. The single variable coefficients of prognosis are calculated as follows

$$\mathrm{CoP_i} = \mathrm{CoP} \cdot \tilde{S}_{\mathrm{T_i}}$$

with the total sensitivity indices

$$\tilde{S}_{\mathrm{T_i}} = 1 - \frac{V_{x_{\sim i}}(E_{\mathrm{x_i}}(\tilde{y} \mid x_{\sim i}))}{V(\tilde{y})}$$

which have been introduced in *Homma and Saltelli (1996)*, where $E_{\mathrm{x_i}}(V(\tilde{y}|x_{\sim i}))$ is the remaining variance of $\tilde{y}$ that would be left, on average, if the parameter of x_{i} is removed from the model. In the equation shown above, $x_{\sim \mathrm{i}}$ indicates the remaining set of input variables. In order to estimate the first order and total sensitivity indices, a matrix combination approach is very common *Most (2012)*.

Optimization process in this work

The process of the optimization is shown in the Fig. 6. First before each component gets optimized, a sensitivity analysis is performed to determine the sensitive parameters for each output parameter and their correlations. Therefore a Latin hypercube sampling (LHS) is made with N = 2 · (Inputparameters + Outputparameters) designs calculated. That means there were 107 designs for the rotor optimization, 83 designs for the diffuser optimization and 130 for the coupled optimization. The Latin hypercube sampling is a advanced method of the monte carlo simulation, which made equal distributed designs in their parameter space. Following that,

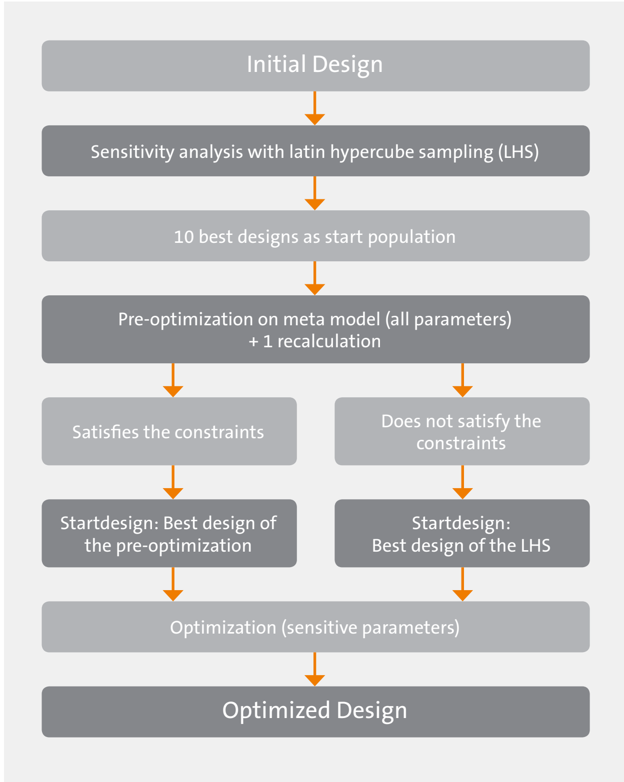

Fig. 6: Overview of the optimization process

a pre-optimization is based on the information of the Latin hypercube sampling creating a meta-model. That means the meta model will be created through the information of the calculated design in the Latin hypercube sampling. The 10 best designs of the Latin hypercube sampling are selected as the starting population for an evolutionary optimization algorithm with all parameters available for each component. These calculations are not carried out in ANSYS, but on the basis of the meta-model. Therewith, it is possible to calculate in a few minutes many designs, to obtain a better design without the use of time expensive calculations. Subsequently, the best design of the pre-optimization will be selected and recalculated in ANSYS. If this design fulfils the constraints it will be used as a start design for a adaptive response surface method (ARSM) optimization, but this time each design is calculated in ANSYS and only sensitive parameters for the respective objective functions and constraints are active. This recalculation depends on how good the meta model is. So it might be possible, that some output have a deviation in the recalculation. If then the constraints are violated this design can not be chosen as a start design for the following optimization. In this case the best design of the LHS will be taken for the further optimization. Possible reasons for such deviations are e.g. strong non-linear physical behaviours or problems with meshing or wrong simulation settings. The prognosis ability is made through a so called coefficient of prognosis (CoP), which gives a percentage value of how good is the output value describable through the input variables. If these values are rather low (≤ 50) it can be expected, that the recalculation will have strong deviations.

Type	Description	Formula	Unit
Constraint	$(h_{\mathrm{in\_h}} - h_{\mathrm{in\_l}}) \cdot 1,2 \ge l_{\mathrm{max}}$	$u_1(\mathbf{d}) = (h_{\mathrm{in\_h}} - h_{\mathrm{in\_l}}) \cdot 1,2 - l_{\mathrm{max}} \ge 0$	[m]
Constraint	$\frac{(2 \cdot \pi \cdot h_{\mathrm{out}} \cdot l_{\mathrm{out}})}{((h^2_{\mathrm{in\_h}} - h^2_{\mathrm{in\_l}}) \cdot \pi)} \ge 2$	$u_2(\mathbf{d}) = \frac{(2 \cdot \pi \cdot h_{\mathrm{out}} \cdot l_{\mathrm{out}})}{((h^2_{\mathrm{in\_h}} - h^2_{\mathrm{in\_l}}) \cdot \pi)} - 2 \ge 0$	$[m^2]$
Constraint	$t_{\mathrm{LE\_**}} \ge t_{\mathrm{TE\_**}}$	$u_3(\mathbf{d}) = t_{\mathrm{LE\_**}} - t_{\mathrm{TE\_**}} \ge 0$	[m]
Constraint	$\lvert f_{i\mathrm{th}} \rvert$ needs to be at least $5s^-1$ away of $f_{0\mathrm{th}}$	$u_4(\mathbf{d}) = \lvert f_{i\mathrm{th}} - f_{0\mathrm{th}} \rvert - 5 \ge 0$	$[s^{-1}]$
Constraint	$\gamma_{\mathrm{r}} \ge 1.5$	$u_5(\mathbf{d}) = \gamma_{\mathrm{r}} - 1.5 \ge 0$	
Constraint	$\gamma_{\mathrm{eqv}} \ge 1.5$	$u_6(\mathbf{d}) = \gamma_{\mathrm{eqv}} - 1.5 \ge 0$	
Objective	Total isentropic stage efficiency η_{st}	$f_1(\mathbf{d}) = \frac{\frac{T_{\mathrm{ex,1}}}{T_{\mathrm{in,0}}} - 1}{(\frac{p_{\mathrm{ex,1}}}{p_{\mathrm{in,0}}})^{\frac{\kappa-1}{\kappa}} - 1}$	
Objective	Specific performance $P/\dot{m}_{\mathrm{in}}$	$f_3(\mathbf{d}) = \frac{2 \cdot \pi \cdot M \cdot f_{0\mathrm{th}}}{\dot{m}_{\mathrm{in}}}$	$[Jkg^{-1}]$

Tab. 1: Constraints $u_m(\mathbf{d})$ and objective $f(\mathbf{d})$

Symbol	O_{init}	O_{pre}	O_{fin}	Unit
AR	1,44	1,44	1,44	
$P/\dot{m}_{\mathrm{in}}$	1,415e5	1,431e5	1,395e5	$[Jkg^{-1}]$
c_{pr}	0,579	0,561	0,435	
$\dot{m}_{\mathrm{in}}$	76,636	77,075	77,126	$[kgs^{-1}]$
η_{st}	0,867	0,879	0,886	
σ_{r}	7,948e8	8,811e8	8,661e8	N/m^2
σ_{eqv}	8,287e8	8,087e8	7,931e8	N/m^2
γ_{eqv}	1,553	1,591	1,622	
γ_{r}	1,577	1,434	1,469	
f_1	82,97	83,75	85,09	$[s^{-1}]$
f_2	190,55	181,25	177,56	$[s^{-1}]$
f_3	174,13	231,82	232,54	$[s^{-1}]$

Tab. 2: Overview for each optimization step after the final optimization of the rotor blades

In the following, this procedure will be repeated, for the rotor, diffuser and the coupled system. The constraints for the optimization regarding the geometry of the blade and diffuser are resulted mainly from the industry through guidelines. Additional constraints were safety factors for the stresses and a minimal distance of the eigenfrequencies to the machine frequency. For the objective the were two Output used. First for the rotor optimization the total isentropic stage efficiency and second for the diffuser and coupled optimization the specific performance as shown in Tab. 1.

Sequential optimization work flow

As the first step the optimization of the rotor blades is realized. Which means that the parameters of the diffuser are deactivated for this process. In Fig. 7 the parametrization for the blade is shown. According to five profile sections with eight parameters, in total 40 parameters for the blade optimization are given. The leading and trailing edge are described through two radii, which result out of the other parameters. The target of this first optimization process is to maximize the isentropic stage efficiency η_{st}.

As a result of the sensitivity analysis, the coefficients of prognosis can be used to measure the importance of the input variables. One example is shown in Fig. 8 for the isentropic stage efficiency. The largest variance of the efficiency is described by the profile at 75% of the blade span. Fig. 9 shows the meta-model of the total isentropic stage efficiency in the subspace of the most important parameters.

The results after the adaptive response surface method optimization and the preoptimization in comparison to the initial design are shown in Tab. 2 with an increasing of the efficiency of nearly 2% in addition to compliance with the constraints.

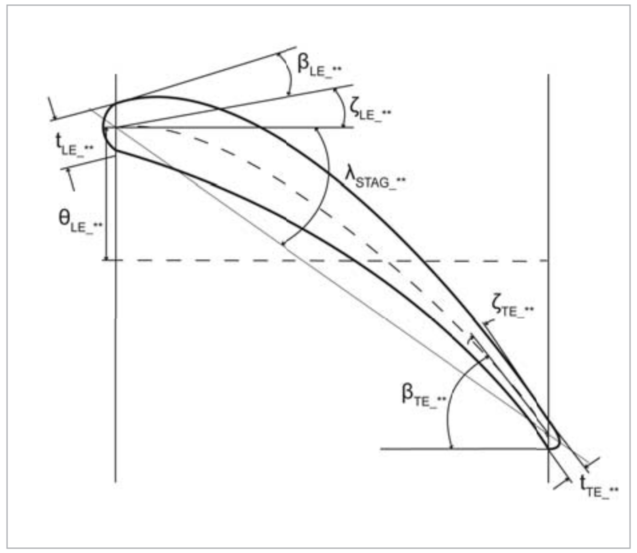

Fig. 7: Overview of the rotor parametrization

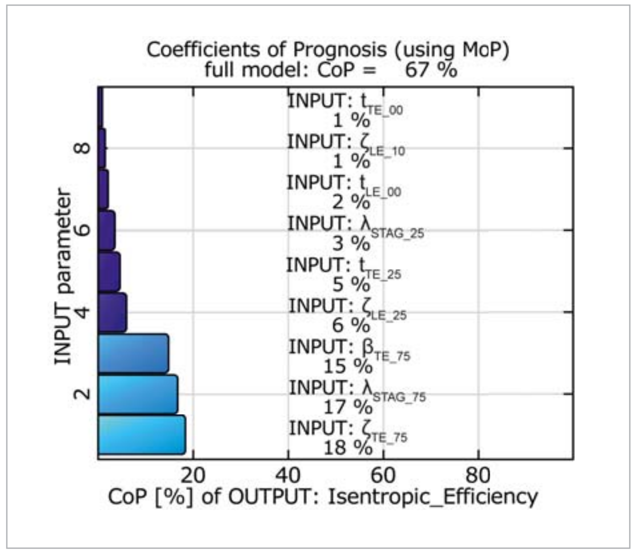

Fig. 8: Most important parameters for the total isentropic stage efficiency

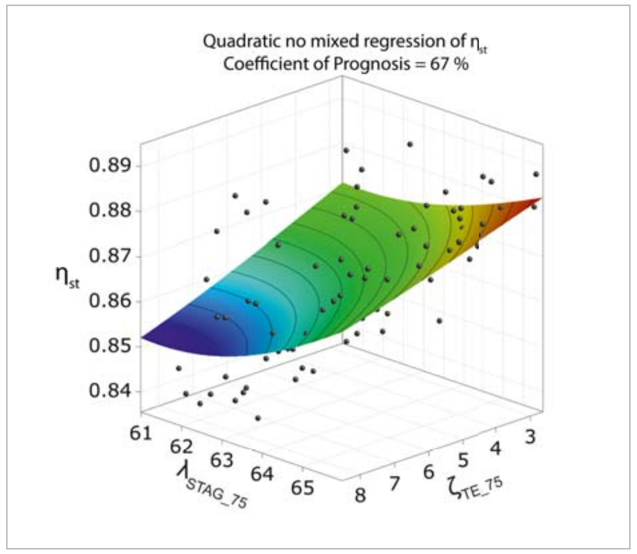

Fig. 9: Total isentropic efficiency and the most important parameters

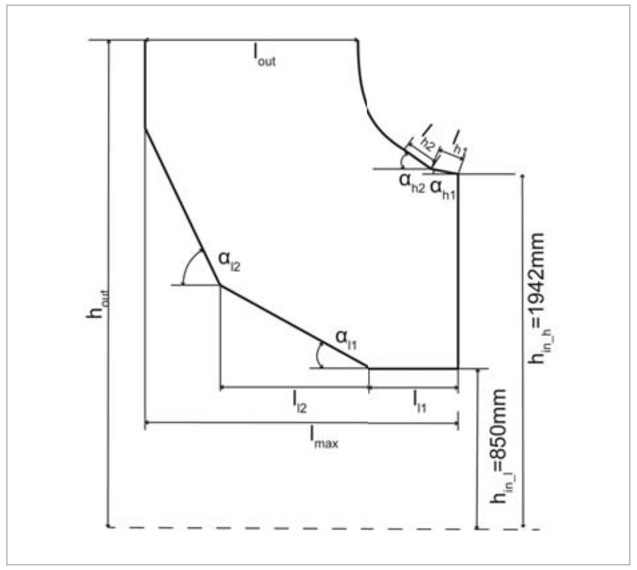

Fig. 10: Diffuser parametrization

Symbol	Metamodel	Recalulation	Difference	Unit
$P/\dot{m}_{\text{in}}$	1,415e5	1,431e5	1,395e5	$[Jkg^{-1}]$
c_{pr}	0,579	0,561	0,435	

Tab. 3: Differences between meta-model and recalculation of the diffuser preoptimization

After the blade optimization, the diffuser optimization is performed. Fig. 10 shows the parametrization. Therefore, 11 parameters are used for the diffuser optimization. The objective for this optimization was the specific performance, because now the optimizer should reach the best performance out of both components with changing the diffuser parameters. It has also been possible to take the pressure recovery as the objective because performance and pressure recovery are correlated. As already described, a preoptimization was carried out based on a meta-model, for each optimization. Table 3 shows as an example of the very small differences between the approximated calculation and recalculation demonstrated on the diffuser pre-optimization. So that this method is a useful tool to perform fast calculations under some circumstances with great improvements as presented here.

Symbol	O_{init}	O_{pre}	O_{fin}	Unit
AR	1,44	1.384	1,417	
$P/\dot{m}_{\text{in}}$	1,395e5	1,416e5	1,418e5	$[Jkg^{-1}]$
c_{pr}	0,435	0,478	0,508	
$\dot{m}_{\text{in}}$	77,126	77,075	77,174	$[kgs^{-1}]$
η_{st}	0,886	0,884	0,883	

Tab. 4: Overview for each optimization step after the final optimization of the diffuser

The final results of the diffuser optimization and thus the sequential optimization are shown in Tab. 4. This time the initial designs stand for the optimized design of the rotor optimization. The resulting increasing of the specific performance is very low, because it is not possible for the optimizer to get a better design out of diffuser optimization. The diffuser is limited to the fixed flow field of the last stage. This means, it is just possible to get a more improved specific performance with changing the flow field in the diffuser. This is reached in this case through increasing the pressure recovery. But as shown there is not a lot of further potential available.

Symbol	O_{init}	O_{pre}	O_{fin}	Unit
AR	1,44	1,44	1,46	
$P/\dot{m}_{\text{in}}$	1,415e5	1,431e5	1,445e5	$[Jkg^{-1}]$
c_{pr}	0,579	0,561	0,571	
$\dot{m}_{\text{in}}$	76,63	77,07	77,29	$[kgs^{-1}]$
η_{st}	0,867	0,879	0,885	
σ_{r}	7,948e8	8,811e8	8,352e8	N/m^2
σ_{eqv}	8,287e8	8,087e8	8,403e8	N/m^2
γ_{eqv}	1,553	1,591	1,531	
γ_{r}	1,577	1,434	1,501	
f_1	82,97	83,75	84,26	$[s^{-1}]$
f_2	190,55	181,25	173,46	$[s^{-1}]$
f_3	174,13	231,82	216,43	$[s^{-1}]$

Tab. 5: Overview for each optimization step after the final optimization of the coupled optimization

Coupled optimization work flow

The last step is the coupled optimization of the rotor and diffuser. Now, the specific power is used as the optimization target. The optimization results are presented in Tab. 5. As shown in this table the specific performance is much better in comparison with the sequential optimization. The optimizer reaches the same level of stage efficiency like the sequential optimization but with keeping the pressure recovery as it was in the initial design. That means with the possibility of changing all parameters, the optimizer could change them in a way that both components benefit. This clearly shows the advantage of the coupled optimization compared to the sequential optimization.

d_o	O_{rot}	O_{dif}	O_{cp}
$P/\dot{m}_{\text{in}}$	$\lambda_{\text{STAG\_75}}$ $t_{\text{LE\_75}}$ -	l_{out} h_{out} l_{max}	$\lambda_{\text{STAG\_75}}$ l_{out} -
c_{pr}	$\lambda_{\text{STAG\_75}}$ $\lambda_{\text{STAG\_10}}$ $t_{\text{LE\_75}}$	l_{out} h_{Out} -	$\lambda_{\text{STAG\_75}}$ h_{Out} $\lambda_{\text{STAG\_50}}$
η_{st}	$\zeta_{\text{TE\_75}}$ $\lambda_{\text{STAG\_75}}$ $\beta_{\text{TE\_75}}$	h_{out} - l_{out}	$\lambda_{\text{STAG\_75}}$ $\beta_{\text{TE\_75}}$ $\zeta_{\text{TE\_75}}$

Tab. 6: Overview of the sensitive parameters in the individual optimization steps

Interpretation of results

Table 6 shows an overview of the different output variables and their sensitive parameters in descending order of importance, depending on the optimization steps. Many of the sensitive parameters of the rotor optimization can also be found in the coupled optimization again. Similarly, the same for the significant parameters of the diffuser optimization. Which means that irrespective of whether a coupled or sequential optimization is made, the same key parameters are identified. Maybe, non-observance of diffuser parameters in the rotor optimization will result in wasting of optimization potential. In the sequential optimization there were much more parameters, for example for the blade optimization, taken as really needed, because most of them have got a much lower effect on the objective as in comparison with only one additional parameter of the diffuser, as shown in this table. Furthermore, this overview shows a certain dominance of the influence of parameters on the performance of the blade and the pressure recovery, which also depend on the diffuser. For the comparison of each column the main parameters of the diffuser optimization move under the main parameters of the rotor results in the optimization of the coupled optimization.

Thus, a further advantage of the coupled optimization is to determine the parameters with the greatest impact in the overall system to develop or to exhaust the full potential for a better performance. Therefore, in Tab. 7 the comparison of sequential and coupled optimization of the relevant output parameters and the constraints is also shown. The result is a specific performance advantage for coupled optimization of 1.8 % compared to the sequential optimization. Furthermore, the pressure recovery with +12.4% and the stage efficiency with +0.2% are better than the sequential optimization results. Only the safety factor of the coupled optimization regarding the von Mises stress is worse at -5.94% as in the sequential optimization, but meet the constraints of ≥ 1.5. Clearly visible is the large influence of a better pressure recovery on the specific power, although there is almost the same stage efficiency for both optimization sequentially and coupled. It should also be noted that only a single parameter (lout) was active in the ARSM of the coupled optimization. One parameter from the diffuser may be enough, to change along with the blade parameters in order to achieve a better overall result.

	$P/\dot{m}_{\text{in}}$	η_{st} (%)	c_{pr}	γ_{eqv}	γ_{r}
O_{seq}	1,418e5	88,3	0,508	1,622	1,469
O_{cp}	1,445e5	88,5	0,571	1,531	1,501
Δ in %	1,8	0,2	12,4	-5,94	2,1

Tab. 7: Differences between the output parameters of sequential and coupled optimization

As a further result, as shown in Fig.s 11-12 and 13-14, the total pressure and velocity profiles in the diffuser inlet and outlet of each optimization step is given for comparison. The overall pressure and velocity distribution in the inlet is nearly equal for all three versions of the diffuser. In the outlet, the distribution of the pressure and velocity of the initial design was much more uniform as it was for the coupled and sequential version. Even so the results for the pressure recovery showed that the initial design and the

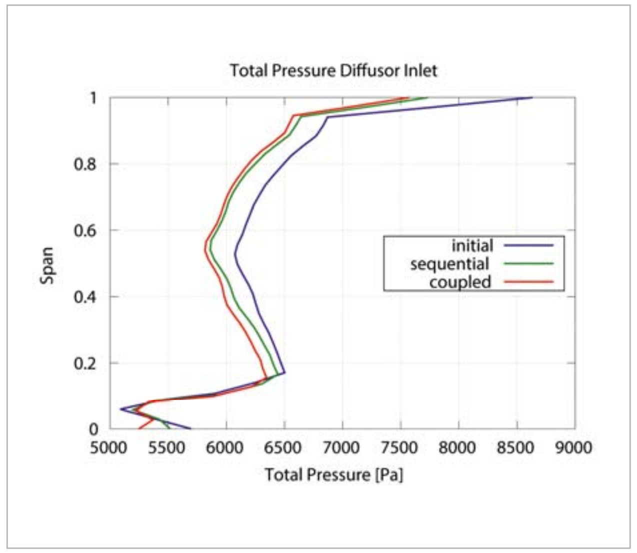

Fig. 11: Pressure profiles in the diffuser inlet of each optimization step

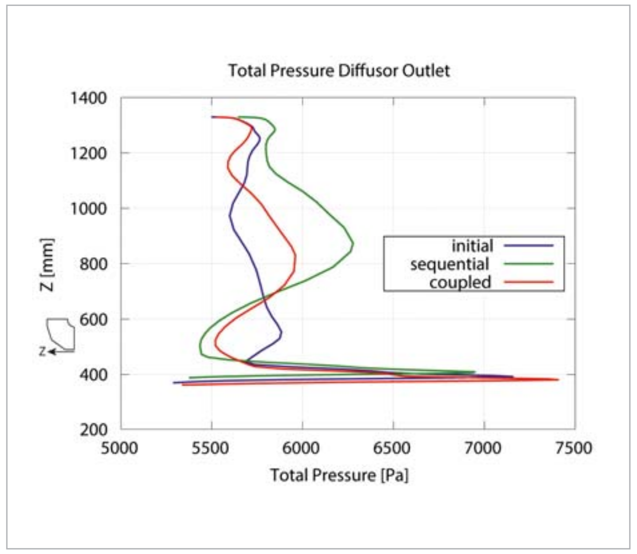

Fig. 12: Pressure profiles in the diffuser outlet of each optimization step

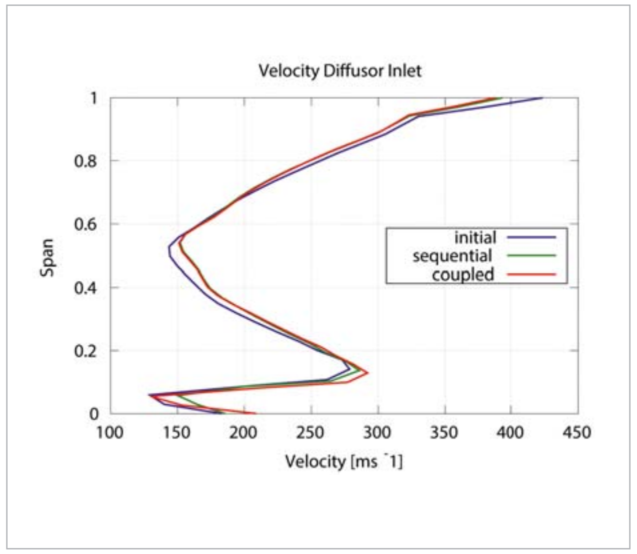

Fig. 13: Velocity profiles in the diffuser inlet of each optimization step

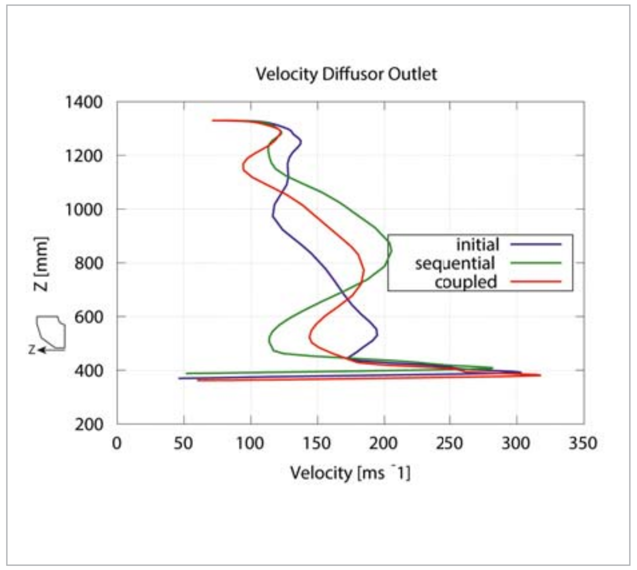

Fig. 14: Velocity profiles in the diffuser outlet of each optimization step

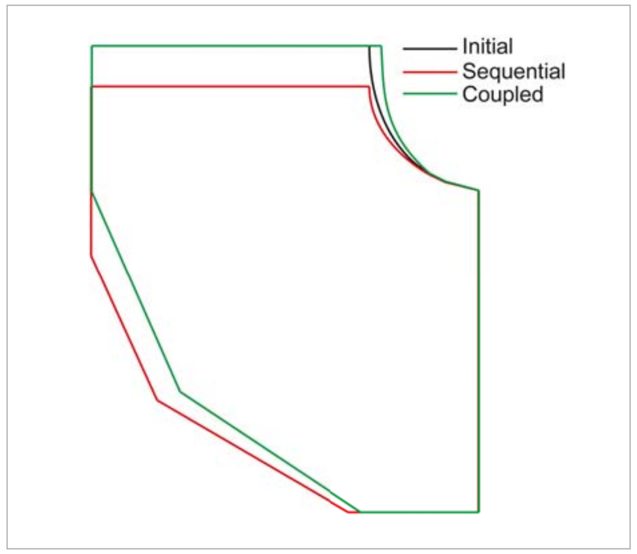

Fig. 15: Superimposed view of the diffuser geometries in the individual optimization steps

coupled optimized design got nearly the same value. The pressure recovery of the sequential optimized design was more worst. This can also be seen in this diagrams. The reduced velocity, which is the result of a diffuser to transfer the kinetic energy into potential energy, is much better for the initial and coupled optimized design. There is a high peak of velocity in the sequential optimized version. So the integral of these curves is much higher for the sequential version as it is for the others, which leads to a overall lower pressure recovery regarding that all three got nearly the same inlet conditions.

Fig. 15 shows the scaled form of the different diffuser geometries. In total 313 designs are calculated with a duration of 33 days and for the coupled optimization and 263 designs with a duration of 28 days for the sequential optimization. As hardware two computers with following specifications are used:

- CPU: 2 x AMD Opteron 6376 with 16 cores, 2.3 GHz
- 64 GB of memory

This computational effort shows whether it makes sense to perform an optimizations using 3D calculations or whether it would be better to use 2D calculations or similar replacement model. The computation efforts for both paths are very long and would probably be too time consuming for use in practice. However, the presented method with a less computationally intensive model or equivalent model and subsequent recalculation in 3D could also be a time efficient way to improve the development of such machines.

Conclusion

The specific performance benefit of the coupled optimization over the sequential optimization is 1.8% in compliance with all constraints. This is mainly explained through a much better interaction between stage and diffuser. In both optimization methods, a similar high stage efficiency is achieved. However, in the sequential optimization in a way that it prevented the diffuser, to reach a much better overall performance, which is below the overall performance of the coupled optimization. In the coupled variant the same efficiency is achieved, but in such a way that the diffuser could also achieve a very high pressure recovery. During the optimizations the whole parameter space, which is used for both, is equal. Therefore, it can be seen as the final result that the coupled optimization in this work has significant advantages over the sequential. The fact that there is a coupling of the two components since the outlet of the stage and thus the flow field corresponds to the field entry of the diffuser. Both have influence on the performance values of the overall system. Although the flow can be designed that it produces a good stage efficiency for the output stage, but a poor flow field for the diffuser and vice versa.

To give this work a conclusion, there is a recommendation to develop and optimize the last stage and the diffuser in a coupled way to use the full potential of both because:

1. There is a better understanding possible of the relationship of individual performance output parameters and the parameters affecting them across the component boundaries.

2. It can be exhausted additional potential, by simultaneous modification of parameters of both components to a better overall performance.

3. The flow field is adjusted, therewith both components can benefit and not a component is better or worse.

4. It may be more time efficient to develop both components simultaneously.

The authors would like to express their thanks to C. Musch of the Siemens AG for his assistance of collaborative method implementation into the CAE process.

Authors // K. Cremanns / D. Roos, A. Graßmann (Niederrhein University of Applied Sciences)

Source // www.dynardo.de/en/library

Nomenclature

$\dot{m}$	Mass flow of the stage inlet $[kg/s]$
η_{st}	Total isentropic stage efficiency
$P/\dot{m}_{in}$	Specific performance $[Jkg/s]$
c_{pr}	Pressure recovery
σ	Stress
γ	Safety factor
f	Eigenfrequency $[s^{-1}]$
AR	Diffuser outlet area/inlet area
d	Parameter
O	Optimization
h	height
t	thickness
l, Θ	length
P	Pressure
$\alpha, \beta, \lambda, \zeta$	Angle
T	Temperature
CoP	Coefficient of Prognosis
κ	Isentropic exponent
M	Torque

Subscripts

init	Initial
pre	Previous
fin	Final
seq	Sequential
cp	Coupled
rot	Rotor
i	Input
ith	1-3th Eigenfrequency
o	Output
eqv	von Mises equivalent stress
r	Radial stress
in	Inlet
out	Outlet
TE	Trailing edge
LE	Leading edge
STAG	Stagger angle
_**	Span at 0, 25, 50, 75, 100 %
dif	Diffusor
0	Stator inlet
1	Rotor outlet/ Diffuser inlet
2	Diffuser outlet